

Toward a Force Spectroscopy of Polymer Surfaces

Kirill Feldman, Theo Tervoort, Paul Smith, and Nicholas D. Spencer*

Department of Materials, Swiss Federal Institute of Technology,
ETH-Zürich, CH-8092 Zürich, Switzerland

Received March 29, 1997. In Final Form: October 7, 1997

The adhesional forces between a series of polymer film surfaces and chemically well-defined atomic force microscopy tips have been measured and found to depend strongly on the chemical nature of both probe and sample surfaces. For a given series of polymers, the ranking in adhesion strength was markedly different for polar and nonpolar probes, irrespective of the precise chemical composition of those probes. In the case of nonpolar polymers, a correlation of adhesion force with calculations based on the Lifshitz theory of Van der Waals interactions was found. In the case of polar polymers, a reasonable correlation with water-contact angle was observed. The adhesional differences between different probe tips translate into reversals of chemical contrast in high-spatial-resolution lateral force images, when examining polymer blends using chemically different tips, demonstrating the potential of this approach for the nanometer-scale, friction-mediated surface-chemical imaging of polymers. Central to these experiments has been the use of perfluorodecalin as a medium for measuring interactions. Employment of this liquid greatly facilitates measurement of the forces between the probe tip and the polymer surface.

Introduction

Atomic and lateral force microscopy techniques (AFM and LFM) have, since their development in the 1980s,^{1,2} shown considerable promise as methods for nanometer-scale, surface-chemical analysis, since they can provide quantitative, spatially resolved, chemically dependent information on interactions between the scanning probe and sample surfaces. This feature has been exploited by many researchers, using approaches such as chemical modification of probe tips for the recognition of specific surface groups^{3–8} or monitoring the pH dependence of the tip–surface interaction.^{9–11} The majority of such studies have involved self-assembled monolayers (SAMs) on flat gold surfaces,¹² which provide an idealized test surface, presenting a well-ordered, morphology-free, highly concentrated plane of functionality. The usefulness of SAMs as models for polymer surfaces is limited, however, since issues such as complex surface morphology, disorder, mechanical properties, and solvent interactions significantly complicate the issue with real polymers, making chemical imaging extremely challenging.^{6,13,14}

Force–distance measurements with conventional (non-

vacuum) scanning probe microscopes are often performed in a liquid environment in order to eliminate the contribution of capillary forces resulting from water adsorption from the air.¹⁵ Moreover, the liquid environment can be used to tune the Van der Waals forces between the probe and the surface.^{16a} This is a valuable approach that others have used for DNA imaging,^{16b} for example. An important consideration here is the makeup of the van der Waals interaction, which can be calculated from the nonretarded Hamaker constant, A_{total} , and which, in turn, consists of the two terms $A_{\nu=0}$ and $A_{\nu>0}$, corresponding to the dipole–dipole and dipole–induced-dipole contributions and the dispersion (London) contributions, respectively, to the van der Waals interaction. According to Israelachvili's simplification¹⁷ of the Lifshitz theory,¹⁸ these contributions can be calculated for a system where two macroscopic phases interact across a third phase, from the respective static dielectric constants ($\epsilon_1, \epsilon_2, \epsilon_3$) and optical refractive indexes (n_1, n_2, n_3) as follows:

$$A_{\text{total}} = A_{\nu=0} + A_{\nu>0} \approx \frac{3}{4} kT \left(\frac{\epsilon_1 - \epsilon_3}{\epsilon_1 + \epsilon_3} \right) \left(\frac{\epsilon_2 - \epsilon_3}{\epsilon_2 + \epsilon_3} \right) + \frac{3h\nu_e}{8\sqrt{2}} \times \frac{(n_1^2 - n_3^2)(n_2^2 - n_3^2)}{(n_1^2 + n_3^2)^{1/2}(n_2^2 - n_3^2)^{1/2} \{ (n_1^2 + n_3^2)^{1/2} + (n_2^2 + n_3^2)^{1/2} \}} \quad (1)$$

where the electronic absorption frequency, ν_e , is assumed to be equal for all three components ($\nu_e = 3 \times 10^{15}$ Hz). The consequence of this relationship is that a close match between the dielectric constants of the tip, the sample, and the medium leads to a suppression of the first term, with the result that dispersion forces (determined by the optical refractive index) play the dominant role in determining the tip–sample adhesion. In fact, if the refractive index of the intervening medium is intermediate

- (1) Binnig, G.; Quate, C. F.; Gerber, Ch. *Phys. Rev. Lett.* **1986**, *56*, 930.
 (2) Mate, C. M.; Erlandsson, R.; McClelland, G. M.; Chiang, S. *Phys. Rev. Lett.* **1987**, *59*, 1942. Overney, R.; Meyer, E. *MRS Bull.* **1993**, May, 26.
 (3) Frisbie, C. D.; Rozsnyai, L. F.; Noy, A.; Wrighton, M. S.; Lieber, C. M. *Science* **1994**, *265*, 2071.
 (4) Lee, G. U.; Kidwell, D. A.; Colton, R. J. *Langmuir* **1994**, *10*, 354.
 (5) Akari, S.; Horn, D.; Keller, H.; Schrepp, W. *Adv. Mater.* **1995**, *7*, 549.
 (6) Sinniah, S. K.; Steel, A. B.; Miller, C. J.; Reutt-Robey, J. E. *J. Am. Chem. Soc.* **1996**, *118*, 8925.
 (7) Green, J.-B. D.; McDermott, M. T.; Porter, M. D.; Siperko, L. M. *J. Phys. Chem.* **1995**, *99*, 10960.
 (8) Han, T.; Williams, J. M.; Beebe, T. P. *Anal. Chim. Acta* **1995**, *307*, 365.
 (9) Marti, A.; Hähner, G.; Spencer, N. D. *Langmuir* **1995**, *11*, 4632.
 (10) Hähner, G.; Marti, A.; Spencer, N. D. *Trib. Lett.* **1997**, *3*, 359.
 (11) Vezenov, D. V.; Noy, A.; Rozsnyai, L. F.; Lieber, C. M. *J. Am. Chem. Soc.* **1997**, *119*, 2006.
 (12) Bain, C. D.; Evall, J.; Whitesides, G. M. *J. Am. Chem. Soc.* **1989**, *111*, 7155.
 (13) Schönherr, H.; Vancso, G. J. *Polym. Prepr.* **1996**, *37* (2), 612.
 (14) Aimé, J. P.; Elkaakour, Z.; Odin, C.; Bouhacina, T.; Michel, D.; Cuély, J.; Dautant, A. *J. Appl. Phys.* **1994**, *76*, 754.

- (15) Grigg, D. A.; Russel, P. E.; Griffith, J. E. *J. Vac. Sci. Technol. A* **1992**, *10*, 680.
 (16) (a) Hutter, J. L.; Bechhoefer, J. *J. Appl. Phys.* **1993**, *73*, 4123.
 (b) Hansma, H. G.; Sinsheimer, R. L.; Li, M.-Q.; Hansma, P. K. *Nucleic Acids Res.* **1992**, *20*, 3585.
 (17) Israelachvili, J. *Intermolecular and Surface Forces*, 2nd ed.; Academic Press: London, 1992; Chapter 11.
 (18) Lifshitz, E. M. *Sov. Phys. JETP* **1956**, *2*, 73.

between those of the other phases, a negative van der Waals interaction can result.¹⁹

The manipulation of surface forces by suitable choice of medium is central to the experiments in the present study. In the case of polymers, the choice of a suitable medium is greatly restricted by potential interactions, as a solvent, for example, with the polymer surface. In view of these constraints, we have chosen perfluorinated decalin (C₁₀F₁₈) as a measurement medium: Employment of this nonpolar liquid, which displays both a low dielectric constant and a low refractive index and is inert toward most polymers, greatly facilitates the measurement of the dispersion component of the Van der Waals forces between the probe tip and the polymer surface.

Below, we describe a systematic study of AFM-adhesion measurements on polymeric surfaces. We have endeavored to control as many of the complicating parameters on polymer surfaces as possible, such that our AFM adhesion measurements were primarily due to the dispersion component of the Van der Waals and H-bonding interactions between the tip and the polymer surface. Using an embryonic "force spectroscopy" approach, polymers could be distinguished by virtue of their differing hydrophobicities/hydrophilicities or, for purely hydrophobic systems, on the basis of their optical refractive index. By capitalizing on the intimate relationship between adhesion and friction,²⁰ these phenomena can be rendered visual by means of lateral force microscopy (LFM), enabling high-spatial-resolution chemical imaging of heterogeneous polymer systems—a challenging analytical task for conventional ultrahigh vacuum surface chemical imaging methods.

Experimental Section

Sample Preparation. A first series of thin (hydrophobic) polymer films consisted of polystyrene, PS (average MW = 250 000, Polysciences, Inc., Warrington, PA), isotactic polypropylene, i-PP (average MW = 250 000, Aldrich Chemical Co., Inc., Milwaukee, WI), poly(vinylidene fluoride), PVDF (average MW = 534 000, Aldrich Chemical Co., Inc., Milwaukee, WI), and poly(tetrafluoroethylene-co-hexafluoropropylene), FEP (Polymer Technology Group, ETH-Zürich).

A second series of thin films consisted of glassy polymers with different hydrophobicities/hydrophilicities: polystyrene, PS (average MW = 250 000, Polysciences, Inc.), polyacrylonitrile, PAN (average MW = 500 000, Polysciences, Inc.), poly(methyl methacrylate), PMMA (average MW = 350 000, Aldrich Chemical Co., Inc.), and poly(acrylic acid), PAA (average MW = 450 000, Aldrich Chemical Co., Inc.).

i-PP, PVDF, and FEP were first prepared from foils made by pressing powders between aluminum sheets above their corresponding melting temperatures. The films obtained were then pressed between plasma-cleaned silicon wafers (once again, above their melting temperatures) to achieve low surface roughness. It must be noted, however, that, due to the crystallization of isotactic polypropylene and PVDF upon cooling, the attainment of a comparable surface roughness to that of the silicon wafer was not anticipated; nevertheless, film roughnesses of ≈ 3 nm were attained. In addition, these polymers have glass transition temperatures of about -22 and -38 °C, respectively, meaning that additional chain rearrangements and an increase in crystallinity may take place during their subsequent storage at room temperature.

Thin films of the other polymers were prepared by spin casting 2 wt % solutions (PS and PMMA in toluene, PAN in *N,N*-dimethylformamide, and PAA in methanol) onto plasma-cleaned

silicon wafers at 1000 rpm, followed by drying in a vacuum oven at 120 °C and 0.03 mbar for 24 h. All polymers of the second series are fully or highly amorphous and have glass transition temperatures of approximately 100 °C. Annealing above T_g ensured low surface roughness of the films and evaporation of the solvents. The thicknesses of the produced films were on the order of 50–100 μm , as measured by ellipsometry. The measured surface roughness of all films was close to that of the silicon substrates.

Probes. Two classes of AFM probe-tip surfaces were used in this work: polar and nonpolar. Polar tips were either oxygen-plasma-treated Si₃N₄ Microlevers (Park Scientific Instruments, Sunnyvale, CA) or Si₃N₄ cantilevers (Digital Instruments, Santa Barbara, CA) with attached COOH-functionalized glass spheres (Bioforce Laboratory, Ames, IA). The nonpolar tips were either gold-coated Si₃N₄ Microlevers or Si₃N₄ cantilevers with attached ≈ 7.5 μm diameter polystyrene beads (Bioforce Laboratory). Sharpened Microlevers were chosen because of their low spring constants (down to 0.007 N/m), providing high sensitivity to the measured pull-off forces and a small (10–20 nm, according to manufacturer's specifications) tip radius. Spring constants of the oxygen-plasma-treated and gold-coated Microlevers were calibrated by the method developed by Cleveland *et al.*²¹ Oxygen-plasma treatment of the Microlevers was carried out in a radiofrequency plasma cleaner (Harrick Scientific Corp., Ossining, NY) operated at 40 W with an oxygen feed. The isoelectric point of the resulting tips was at approximately pH ≈ 3 (measured by the method of Marti *et al.*⁹), suggesting that the surface consisted chiefly of SiO_x. The gold-coated tips were prepared by thermal deposition of a 4 nm chromium adhesion layer, followed by 20 nm of gold in a Balzers (Liechtenstein) MED 010 coater operated at 2×10^{-5} mbar. A single tip of each type was used to measure all polymer surfaces within a given series, to ensure that the spring constant and tip radius were kept constant between samples.

Measurements. Force–distance measurements and lateral force imaging were performed with a scanning probe microscope (Nanoscope III Multimode, Digital Instruments) equipped with a liquid cell and enclosed in a thermally equilibrated environment. Up to 1280 force–distance curves at adjacent locations were collected for each sample. Prior to the measurements, the films were briefly placed under an α -radiation source, ²¹⁰Po (NRD, Inc., Grand Island, NY) to ensure that the static charge, which is likely to be present on the polymer surfaces, was removed and did not contribute to the overall forces measured. Following each set of experiments on a given series of polymers, the initial measurements were repeated, in order to check that the tip was unaltered and intact. Reproducibility was found to be within 15%.

In order to determine the influence of time dependent effects on the pull-off force for the polymer systems investigated, both load-dependent and frequency-dependent experiments were carried out (0.25–5.5 nN applied load and 0.1–5 Hz for loading–unloading cycles). No significant load dependence was detected over the investigated range, while the pull-off force was found to decrease by $\approx 25\%$ over the measured frequency range, largely due to an increasing loading–unloading hysteresis. We decided to perform measurements at low frequency (0.5 Hz), below the onset of hysteresis.

Refractive index and film thicknesses were measured by ellipsometry (Type L-116 C, Gaertner Science Corp., Chicago, IL) using a 70° angle of incidence and a He–Ne laser. Static water-contact angle measurements were carried out using a contact angle goniometer (Ramé-Hart, Inc., Mountain Lakes, NJ).

We chose perfluorodecalin (PFD), C₁₀F₁₈, (Fluorochem, U.K.) as a medium for all AFM and LFM experiments, both for the reasons discussed in detail above and because PFD is not a solvent for any of the materials examined in this study. Additionally, PFD is convenient to use in AFM experiments because of its relatively low vapor pressure ($P_v = 0.88$ kPa), high boiling point ($T_b = 141$ °C), and nontoxicity.

(19) Burnham, N. A.; Colton, R. J. Force Spectroscopy. In *Scanning Tunneling Microscopy and Spectroscopy: Theory, Techniques, and Applications*; Bonnell, D. A., Ed.; VCH Publishers, Inc.: New York, 1993; Chapter 7.

(20) Israelachvili, J. N.; Chen, Y.-L.; Yoshizawa, H. *J. Adhesion Sci. Technol.* **1994**, *8*, 1234.

(21) Cleveland, J. P.; Manne, S.; Bocek, D.; Hansma, P. K. *Rev. Sci. Instrum.* **1993**, *64*, 403.

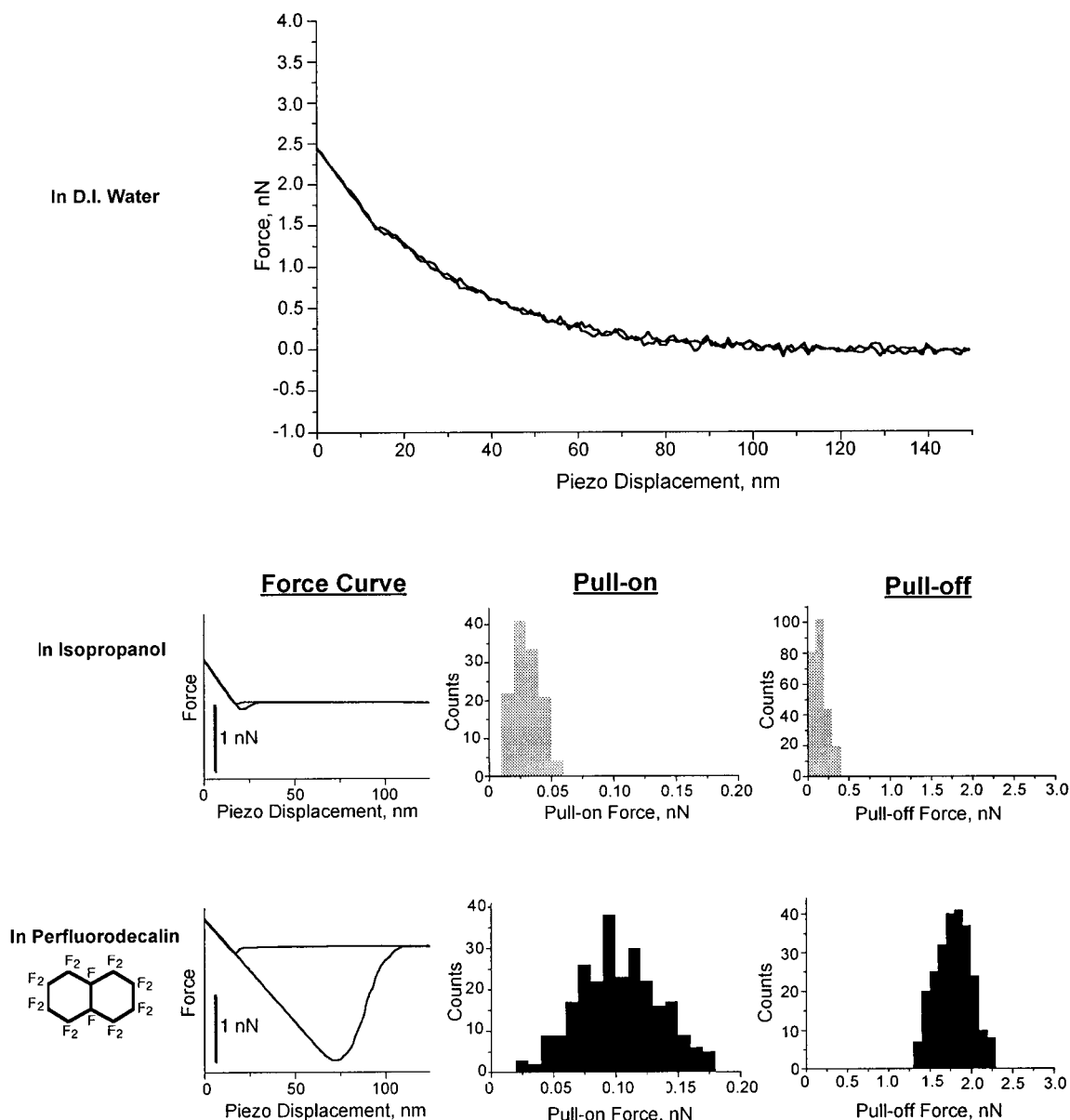


Figure 1. Comparison of force curves and pull-on and pull-off forces between a SiO_x probe and a PMMA surface in water, 2-propanol, and perfluorodecalin.

Table 1. Calculated and Measured Values for Interactions between the First Series of Polymers and a SiO_x Probe ($R = 51$ nm from Figure 3)

polymer	measured refractive index (n)	dielectric constant (ϵ)	$A_{v=0}$, $\text{J} \times 10^{21}$	$A_{v>0}$, $\text{J} \times 10^{21}$	A_{Total} , $\text{J} \times 10^{21}$	calcd work of adhesion, mN/m	calcd pull-off force (JKR), nN (ranking)	measured pull-off force, nN (ranking)
FEP	1.348	2.1	0.17	1.48	1.65	1.6	0.39 (4)	0.18 ± 0.08 (4)
PVDF	1.407	8.4	1.12	4.09	5.21	5.1	1.23 (3)	0.62 ± 0.20 (3)
iPP	1.501	2.5	0.31	8.11	8.42	8.2	1.98 (2)	2.07 ± 0.15 (2)
PS	1.582	2.5	0.31	11.44	11.75	11.4	2.76 (1)	2.98 ± 0.16 (1)

Results and Discussion

An example of the effect of different media on force–distance measurements is shown in Figure 1 for the case of a PMMA surface scanned with a SiO_x probe in water, 2-propanol, and PFD. Since both the PMMA surface and the SiO_x probe are negatively charged at neutral pH, the force–distance measurements in water exhibit strong double-layer interaction forces: Most polymer surfaces acquire a charge in water,²² and this is a common feature

for force–distance measurements for polymers under water using a SiO_x probe. From Figure 1 it is also clear that PFD ($n = 1.317$) leads to a far greater tip–sample interaction (both pull-on and pull-off force) than 2-propanol ($n = 1.378$), when used as the intervening medium between a SiO_x ($n = 1.480$) tip and a PMMA ($n = 1.482$) surface. The higher pull-off forces and therefore greater signal-to-noise ratio obtained in force–distance measurements under PFD thus facilitate comparisons between different polymer samples. Calculations (Tables 1–3) show the interaction to be overwhelmingly dominated by the dispersion component for all polymers used in this study, due to the low refractive index, n , of PFD and the similarity

(22) Garbassi, F.; Morra, M.; Occhiello, E. *Polymer Surfaces: From Physics to Technology*; John Wiley & Sons Ltd: Chichester, 1994; Chapter 1.

Table 2. Calculated and Measured Values for Interactions between the Second Series of Polymers and a SiO_x Probe (*R* assumed to be 20 nm)

polymer	measured water contact angle, deg	measured refractive index (<i>n</i>)	dielectric constant ³³ (ϵ)	$A_{v=0}$, $J \times 10^{21}$	$A_{v>0}$, $J \times 10^{21}$	A_{total} , $J \times 10^{21}$	calcd work of adhesion, mN/m	calcd pull-off force (JKR), nN (ranking)	measured pull-off force, nN (ranking)
PAN	64 ± 2	1.356	6.5	0.99	1.84	2.83	2.8	0.26 (4)	1.32 ± 0.15 (3)
PMMA	68 ± 2	1.482	3.6	0.60	7.31	7.91	7.7	0.73 (3)	1.84 ± 0.16 (2)
PAA	H ₂ O soluble	1.506	5.0	0.83	8.32	9.15	8.9	0.84 (2)	2.13 ± 0.14 (1)
PS	91 ± 2	1.582	2.5	0.31	11.44	11.75	11.4	1.08 (1)	0.66 ± 0.10 (4)

Table 3. Calculated and Measured Values for Interactions between the Second Series of Polymers and a PS Particle (*R* ≈ 3.75 μm) Probe

polymer	measured refractive index (<i>n</i>)	dielectric constant (ϵ)	$A_{v=0}$, $J \times 10^{21}$	$A_{v>0}$, $J \times 10^{21}$	A_{total} , $J \times 10^{21}$	calcd work of adhesion, mN/m	calcd pull-off force (JKR), nN (ranking)	measured pull-off force, nN (ranking)
PAN	1.356	6.5	0.33	2.91	3.24	3.2	55.7 (4)	54.4 ± 20.6 (4)
PMMA	1.482	3.6	0.20	11.57	11.77	11.5	202.6 (3)	112.8 ± 3.9 (2)
PAA	1.506	5.0	0.27	13.17	13.44	13.1	231.4 (2)	75.4 ± 4.5 (3)
PS	1.582	2.5	0.10	18.11	18.21	17.7	313.6 (1)	134.7 ± 7.5 (1)

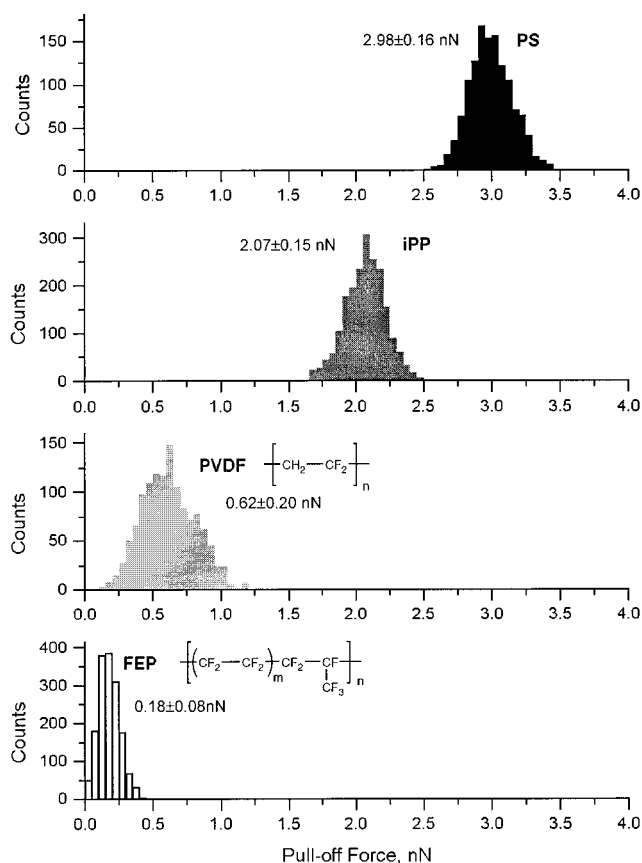
of its dielectric constant, ϵ , to those of the surrounding solid phases.

To explore the use of PFD as a contrast-enhancing medium in force–distance measurements on polymer surfaces, two series of polymers were chosen for the experiments: a first series, consisting of apolar polymers with different refractive indexes, and a second series, in which polymers of different hydrophobicities/hydrophilicities were selected.

First Polymer Series. The first series of polymers was investigated, in order to limit the interaction between an AFM probe and polymer surfaces to only the *dispersion* (London) component of the Van der Waals force. Adhesion forces were measured between a SiO_x probe and a set of nonpolar polymers that provided a range of refractive indexes (as measured): polystyrene (1.582), isotactic polypropylene (1.501), poly(vinylidene fluoride) (1.407), and poly(tetrafluoroethylene-*co*-hexafluoropropylene) (1.348). The histograms of the pull-off forces, measured with a SiO_x probe, are shown in Figure 2 and tabulated with the calculated values for adhesion energy in Table 1.

The Hamaker constants for these systems were derived from eq 1, as described above. The work of adhesion, W , was calculated from the following approximation,¹⁷ $W \approx A_{total}/12\pi D_0^2$, where $D_0 = 0.165$ nm is the commonly used value for the cutoff separation.¹⁷ Plotting measured pull-off forces, F , vs the calculated work of adhesion values, W , should yield a slope of $1.5\pi R$, if the JKR²⁵ theory holds for our system (or $2\pi R$ if DMT²³ is a more appropriate model²⁴). The results (Figure 3) indicate that, for this first polymer series, F scales linearly with W , with a corresponding tip radius (assuming JKR) of ≈ 50 nm. In other words, in the case of nonpolar polymers, AFM pull-off force results obtained under PFD scale quite well with adhesion energies predicted from Lifshitz theory.

Second Polymer Series. Our second series of experiments involved measurements of the pull-off forces in PFD between AFM probes and the surfaces of polymer films with varying degrees of hydrophobicity/hydrophilicity: PS, PAN, PMMA, and PAA. The histograms of the distributions of pull-off forces measured between AFM probes and polymer surfaces in PFD (Figures 4–6) clearly indicate two trends: one for the nonpolar tips (virtually identical results were obtained for both the gold and the polystyrene

**Figure 2.** Histograms of pull-off forces measured between a SiO_x probe and PS, i-PP, PVDF, and FEP surfaces in perfluorodecalin.

probes), where the adhesion is strongest for the polystyrene sample and weakest for poly(acrylonitrile), and the other for the polar probes (again, very similar results being obtained for the SiO_x- and COOH-coated tips), where the strongest adhesion is observed with the poly(acrylic acid) surface and the weakest with polystyrene.

The Hamaker constants and the work of adhesion for the second series were calculated as described above. Pull-off forces were calculated using the JKR theory,²⁵ $F = -1.5\pi WR$, where, for this second set of polymer films, the effective radius, R , of a sharpened tip was given a typical

(23) Derjaguin, B. V.; Muller, V. M.; Toporov, Yu. P. *J. Colloid Interface Sci.* **1975**, *53*, 314.

(24) Burnham, N. A.; Kulik, A. J.; Oulevey, F.; Mayencourt, C.; Gourdon, D.; Dupas, E.; Gremaud, G. In *Micro/Nanotribology and Its Applications*; Bhushan, B., Ed.; NATO ASI Series E: Applied Sciences; Kluwer Academic Publishers: Dordrecht, 1997; Vol. 330, p 421.

(25) Johnson, K. L.; Kendall, K.; Roberts, A. D. *Proc. R. Soc. London A* **1971**, *324*, 301.

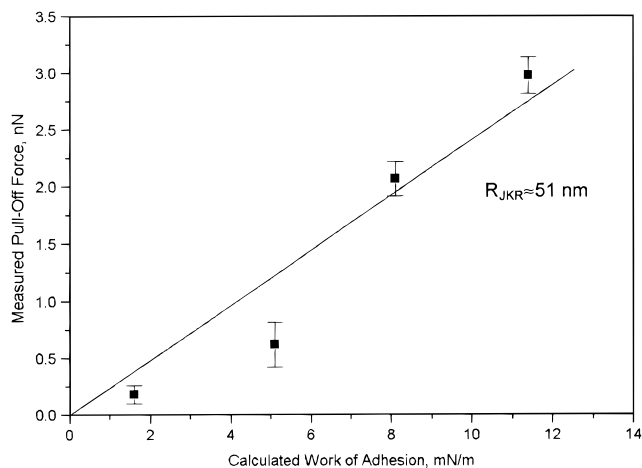


Figure 3. Comparison of measured pull-off forces and the calculated work of adhesion for interactions between a SiO_x probe and PS, i-PP, PVDF, and FEP surfaces in perfluorodecalin.

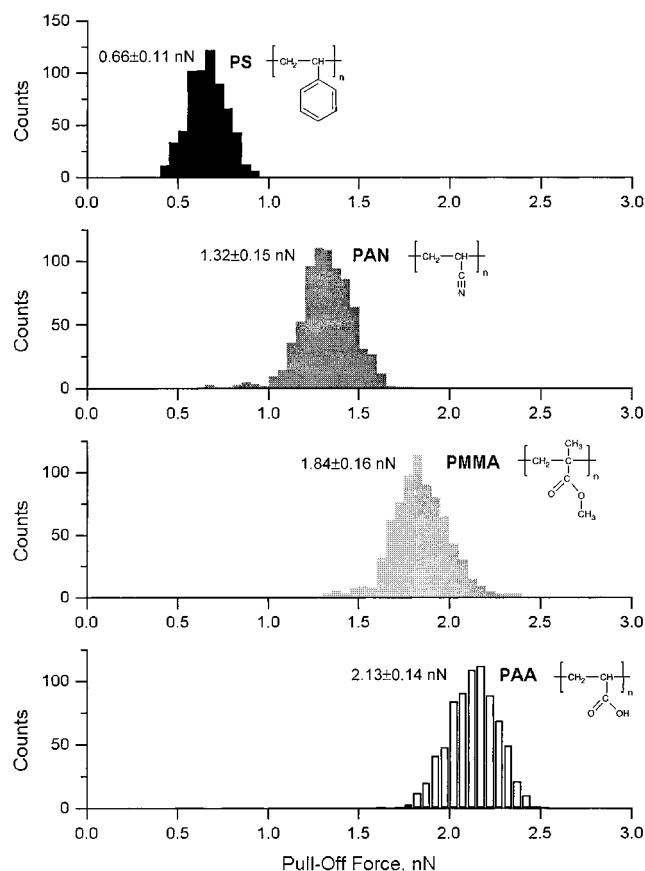


Figure 4. Histograms of pull-off forces measured between a SiO_x probe and PS, PAN, PMMA, and PAA surfaces in perfluorodecalin.

value of 20 nm.²⁶ These results highlight both the promise and the difficulties of this approach to polymer surface characterization. In the case of the nonpolar probes, the measured ranking in adhesion is roughly similar to that calculated for the PS-sphere probe (Table 3). Presumably the surface roughness of the PS-sphere is at least partially responsible for the significant disparities in absolute values. In the case of the polar probes, the measured order of adhesion is entirely different from the values calculated from the Lifshitz theory (Table 2). It must be

(26) Manufacturer's specifications: Park Scientific Instruments, Sunnyvale, CA.

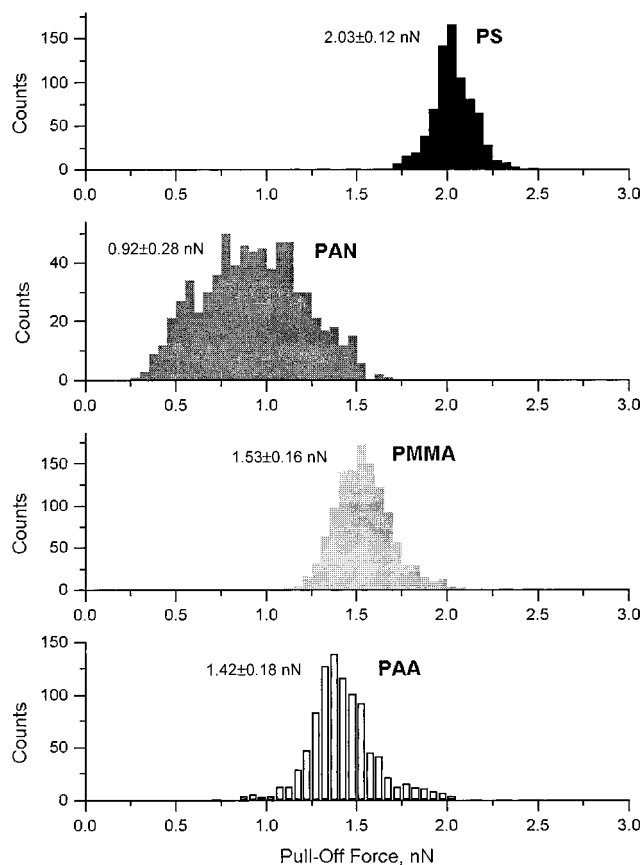


Figure 5. Histograms of pull-off forces measured between a gold probe and PS, PAN, PMMA, and PAA surfaces in perfluorodecalin.

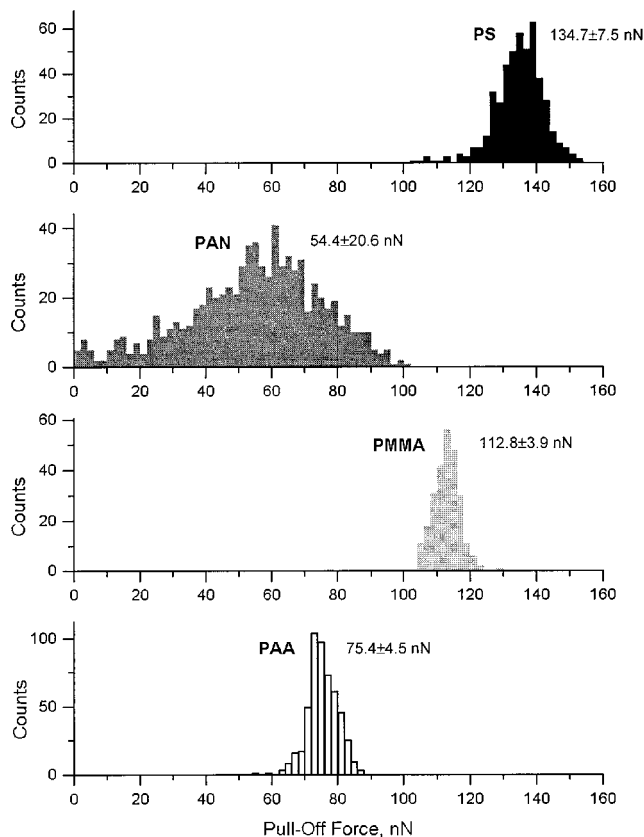


Figure 6. Histograms of pull-off forces measured between a polystyrene sphere (radius 3.75 μm) probe and PS, PAN, PMMA, and PAA surfaces in perfluorodecalin.

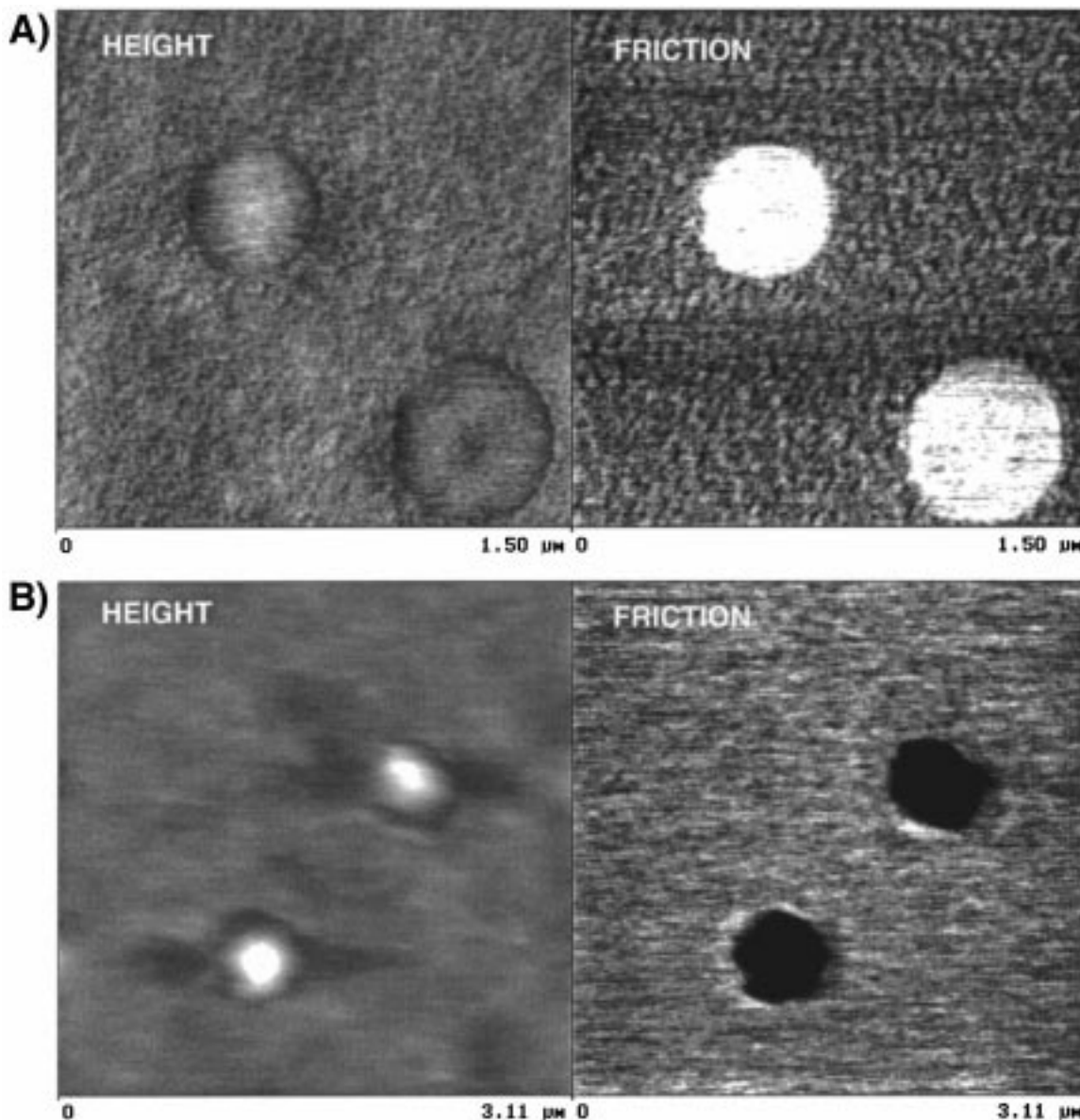


Figure 7. Height (AFM) and friction (LFM) images of a spin-cast polystyrene/poly(methyl methacrylate) polymer blend [PS/PMMA (1:10 w/w)], obtained with (a) gold-coated and (b) SiO_x tips under perfluorodecalin.

borne in mind, however, that many important surface properties of polymers are not taken into account by the calculation: PAA, with its free carboxyl groups, might reasonably be expected to form hydrogen bonds with hydroxyl species on the SiO_x tip. This effect would not, of course, be accounted for in the Lifshitz formalism. In the case of PMMA, which generally displayed strong interactions with both polar and nonpolar probes, surface rearrangement²⁷ could lead to a preferential orientation of either methyl or methacrylate groups toward the interface, depending on the nature of the approaching probe, thus increasing the strength of the interaction in both situations. Although our experiments were carried out at room temperature, some 80 °C below the bulk T_g , simulations by Mansfield and Theodorou²⁸ and experimental work by Kambour²⁹ (rapid craze healing of PMMA at room temperature) show that mobility at the surface

is greatly enhanced over the corresponding bulk value, thus increasing the feasibility of rearrangement. Furthermore, the Van der Waals interaction of PFD with the polymer surfaces (all of which are wetted by PFD) presumably enhances surface mobility. The correspondence between the calculations and the measured interactions between PAN and the nonpolar probes is quite good, providing that the measured (ellipsometric, thin film), rather than the literature (bulk), values for the refractive index are used. The measured refractive index value is lower (1.356) than that in the literature (1.518). Frank *et al.*³⁰ have shown that the physical properties of spin-cast thin polymer films can differ substantially from those of corresponding bulk samples. In particular, these authors observed solvent incorporation to be higher in spin-cast films. This could account for the deviations of our refractive index measurements from literature values, in particular for PAN, where the presence of a small oxygen signal in XPS analysis of the film suggests that traces of solvent (*N,N*-dimethylformamide) were indeed present.

(27) Garbassi, F.; Morra, M.; Occhiello, E. *Polymer Surfaces: From Physics to Technology*; John Wiley & Sons Ltd: Chichester, 1994; Chapter 2.

(28) Mansfield, K. F.; Theodorou, D. N. *Macromolecules* **1991**, *24*, 6283.

(29) Kambour, R. P. *J. Polym. Sci.* **1964**, *2*, 4165.

(30) Frank, C. W.; Rao, V.; Despotopoulou, M. M.; Pease, R. F. W.; Hinsberg, W. D.; Miller, R. D.; Rabolt, J. F. *Science* **1996**, *273*, 912.

By reducing the density, solvent incorporation lowers the refractive index, which, in turn, affects the Van der Waals interaction, as shown in eq 1, and therefore leads to a decrease in the Hamaker constant.

The Lifshitz theory is insufficient to account for the behavior of the second polymer series, in particular when examined with the polar probes. However, since the SiO_x probe is known to contain hydroxyl groups, it was attempted to correlate the adhesion measurements with the behavior of water on the surface as measured by water-contact angle (see Table 2). The water-contact angle measurements were observed to correlate reasonably well with pull-off forces for the second polymer series and the polar probes, suggesting that the AFM-van der Waals approach could potentially be used to provide local hydrophobicity/hydrophilicity information and thus to differentiate between polymer surfaces, as an alternative to the method described by Sinniah *et al.*⁶

Differences in tip radius would account for the difference in the SiO_x -PS pull-off forces derived from the two series of measurements (Figures 2 and 4), given that the spring constants for the cantilevers appeared to be very similar. Imaging the tip used for the first polymer series (tip radius 50 nm) by field-emission scanning electron microscopy showed that it was, indeed, somewhat flattened. The tips for the second polymer series measurements had been taken from a different area of the wafer and were presumably closer to specifications (20 nm). This illustrates another difficulty with attempts to obtain quantitative analytical data with AFM and the need for independent measurements of tip properties.

Frictional Measurements. The histograms in Figures 4 and 5 demonstrate that the chemical nature of the probe tip determines, for example, whether it is PS or PMMA that exhibits the greater adhesional force between the tip and the polymer surface. Given that frictional forces are generally commensurate with adhesion hysteresis²⁰ (which usually varies monotonically with pull-off force), we would also expect to see a reversal of contrast between the two tip classes in LFM (frictional) images of PS-PMMA blends. It is worth noting that, while the bulk elastic moduli of the two polymers are very similar, 3200 and 3300 MPa for PS and PMMA, respectively, frictional contrast between these two polymers has been reported³¹ for an applied load of 10 nN and found to be lower for PS, suggesting that surface nanomechanical properties may vary from those of the bulk. The same

authors observed the reversal of contrast upon decreasing the applied load.³²

We prepared a blend by spin-coating a 2 wt % solution of PS and PMMA (1:10 weight ratio) onto a Si wafer; the resulting film was annealed at 140 °C overnight to ensure substantial phase separation. The film was LFM-imaged in PFD with both SiO_x - and gold-coated tips at zero applied load (the load being due to the work of adhesion only). Both height and frictional (loop-subtracted) images are shown in Figure 7. These images clearly reveal the tip-dependent reversal of the frictional contrast for the two polymers: friction was lower for PS- SiO_x than for PMMA- SiO_x and higher for PS-Au than for PMMA-Au.

Conclusions

The surface nanochemical imaging of polymers with AFM is clearly an analytical challenge, in that the chemically induced properties are convoluted with many other factors, such as disorder, mechanical properties, surface dynamics, and morphology. Nevertheless, when these other factors are carefully controlled, it appears that AFM may be used to distinguish, in the case of nonpolar systems, between areas of differing optical refractive index, as manifested by the London component of the van der Waals force. In the case of polar systems, the approach can distinguish between regions of different hydrophilicity. By imaging in frictional mode (LFM), this same information could be used to provide a high-spatial-resolution chemical map of many heterogeneous polymer systems, especially in cases where the mechanical properties of the components are similar. It was found that, due to its low refractive index, the use of perfluorinated decalin as a medium in AFM experiments significantly enhanced the differences in pull-off forces measured on various polymer surfaces.

Acknowledgment. N.S. and K.F. are grateful for funding from the Council of the Swiss Federal Institute of Technology through their Priority Program on Materials and MINAST program. The authors also wish to acknowledge useful discussions with our colleague, Dr. Nancy Burnham, Ecole Polytechnique Fédérale de Lausanne, and some provocative observations by our anonymous reviewers.

LA9703353

(32) The use of nanomechanical measurements is, of course, an alternative approach to that described in this paper for the chemical imaging of polymers. We believe, however, that it is likely to be more prone to ambiguity, due to the dependence of mechanical properties on processing conditions.

(33) *Polymer Handbook*, 3rd ed.; Brandrup, J., Immergut, E. H., Eds.; J. Wiley & Sons, Inc.: New York, 1989.

(31) Krausch, G.; Hipp, M.; Böltau, M.; Marti, O.; Mlynek, J. *Macromolecules* **1995**, *28*, 260.